H_2 Activation

DOI: 10.1002/anie.201308175

A d^{10} Ni–(H_2) Adduct as an Intermediate in H–H Oxidative Addition across a Ni–B Bond**

*W. Hill Harman, Tzu-Pin Lin, and Jonas C. Peters**

Abstract: *Bifunctional E–H activation offers a promising approach for the design of two-electron-reduction catalysts with late first-row metals, such as Ni. To this end, we have been pursuing H_2 activation reactions at late-metal boratranes and herein describe a diphosphine–borane-supported Ni–(H_2) complex, [(^{Ph}DPB^{iPr})Ni(H_2)], which has been characterized in solution. ^{1}H NMR spectroscopy confirms the presence of an intact H_2 ligand. A range of data, including electronic-structure calculations, suggests a d^{10} configuration for [(^{Ph}DPB^{iPr})Ni(H_2)] as most appropriate. Such a configuration is highly unusual among transition-metal H_2 adducts. The nonclassical H_2 adduct is an intermediate in the complete activation of H_2 across the Ni–B interaction. Reaction-coordinate analysis suggests synergistic activation of the H_2 ligand by both the Ni and B centers of the nickel boratrane subunit, thus highlighting an important role of the borane ligand both in stabilizing the d^{10} Ni–(H_2) interaction and in the H–H cleavage step.*

Although H_2 activation by Ni complexes is well-known,[1] only recently have thermally stable H_2 adducts of Ni been isolated and structurally characterized.[2] The few molecular Ni–(H_2) complexes that have been characterized to date are cationic Ni^{II} species.[2c,d,3] These complexes undergo heterolytic cleavage of the H_2 ligand, whereby an internal or external base removes a proton to deliver hydride to the Ni center. This type of heterolytic cleavage of H_2 figures prominently in a family of synthetic hydrogenase catalysts[4] as well as some molecular hydrogenation catalysts.[5] On the other hand, oxidative addition of H_2 to a single Ni center is virtually unknown, a fact borne out by the absence of stable nickel dihydride complexes. Furthermore, there are no examples of H_2 adducts of zero-valent Ni centers that might subsequently undergo oxidative addition. Strategies to enable this reactivity at zero-valent Ni could widen the scope of reactions catalyzed by this base metal (Scheme 1).

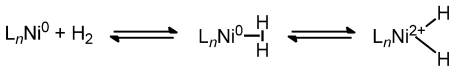

Scheme 1. Schematic representation of H_2 binding and oxidative addition at a reduced Ni center.

We recently reported the reversible cleavage of H_2 by the nickel–borane complex [(^{Mes}DPB^{Ph})Ni] (**1**) to give [(^{Mes}DPB^{Ph})(μ-H)NiH] (**2**; Scheme 2).[6] In a limiting sense, this reaction reverses the polarity of the H_2 heterolysis

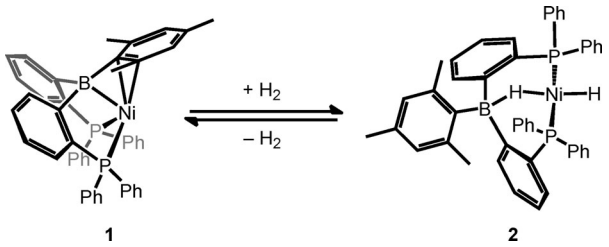

Scheme 2. Reversible H_2 activation by [(^{Mes}DPB^{Ph})Ni] (**1**).

reaction discussed above, with the transition metal acting as a Brønsted base and the borane receiving the hydride. We reasoned that by using more-electron-rich phosphine donors while maintaining the phenyl substituent at boron, we might enhance H_2 binding and impede H–H cleavage to enable the observation of an intermediate H_2 adduct of Ni^0. Observation of such a species would be desirable, as no d^{10} transition-metal adducts of H_2 have been characterized in solution. To this end, we examined a ligand variant with isopropyl substituents at phosphorus, PhB(*o*-*i*Pr$_2$PC$_6$H$_4$)$_2$ (^{Ph}DPB^{iPr}, **3**).[7] Herein we report zero-valent Ni–(N_2) and Ni–(H_2) complexes supported by **3**. The latter complex underwent quantitative oxidative addition of the H_2 ligand across the Ni–B bond. The relatively slow rate of H_2 activation has allowed us to thoroughly characterize this unusual Ni–(H_2) adduct in solution as well as monitor the kinetics of H_2 activation. These data and accompanying computational studies suggest an important role for the B atom, both in H_2 binding and activation.

The red-orange Ni complex [(^{Ph}DPB^{iPr})NiBr] (**4**) was accessed through comproportionation and reduced by Na/Hg in THF to give the diamagnetic, brick-red N_2 complex [(^{Ph}DPB^{iPr})Ni(N_2)] (**5**; Scheme 3). The IR spectrum of a powder sample of **5** featured an intense band at 2152 cm^{-1}, consistent with a weakly activated terminal N_2 ligand. Slow evaporation of a solution of this material in pentane gave deep-red crystals that were shown by X-ray

[*] Dr. W. H. Harman,[+] Dr. T.-P. Lin, Prof. Dr. J. C. Peters
Division of Chemistry and Chemical Engineering
California Institute of Technology (USA)
E-mail: jpeters@caltech.edu

[+] Current address: Department of Chemistry, University of California Riverside, CA 92521 (USA)

[**] This research was supported by the NSF Center for Chemical Innovation: Solar Fuels (grant CHE-0802907) and by the Gordon and Betty Moore Foundation. We thank Prof. Christopher C. Cummins and Dr. Smith Nielsen for insightful discussions.

Supporting information for this article is available on the WWW under http://dx.doi.org/10.1002/anie.201308175.

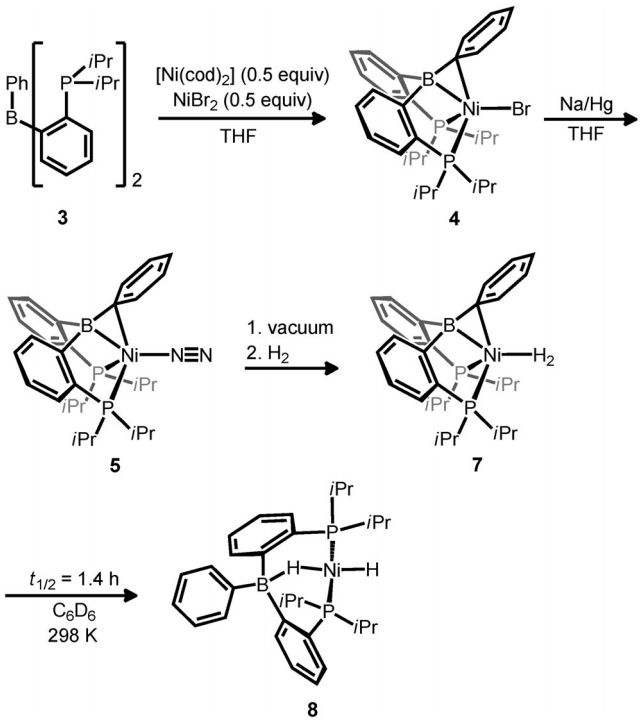

Scheme 3. Synthesis of Ni complexes derived from the diphosphine–borane ligand $^{Ph}DPB^{iPr}$ (**3**). cod = 1,5-cyclooctadiene.

diffraction to contain two crystallographically distinct molecules of **5** and one half of the bridging N_2 complex $[\{(^{Ph}DPB^{iPr})Ni\}_2(\mu\text{-}N_2)]$ (**6**) per asymmetric unit (Figure 1).[8] Each of the three crystallographically distinct Ni centers in the asymmetric unit adopts a pseudotetrahedral geometry featuring a short Ni–(η^2-B,C_{ipso}) interaction in which the boron center remains essentially planar (Table 1). Structurally characterized Ni–(N_2) complexes are relatively rare.[2c,d,9]

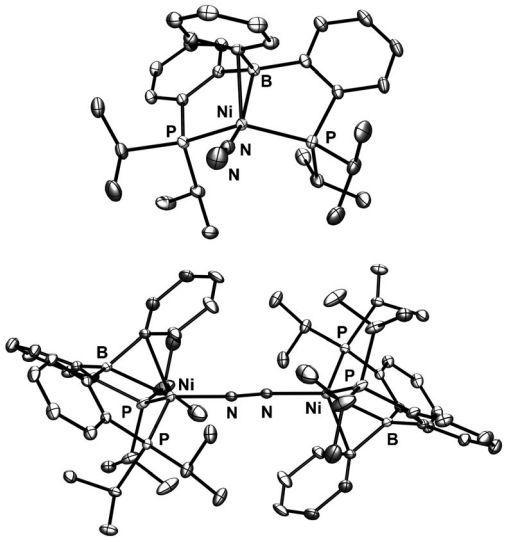

Figure 1. Thermal-ellipsoid plots (50%) of **5** (top) and **6** (bottom). Hydrogen atoms have been omitted for clarity. Both molecules are present within the same crystal (see text).

Table 1: Selected distances [Å] and angles [°] for the two crystallographically distinct molecules of **5** as well as the values calculated by using the indicated functionals with the 6-311++G** basis set.

	X-ray diffraction		B3LYP	M06L
d(Ni–B)	2.2007(17)	2.1807(18)	2.199	2.208
d(Ni–P)$_{avg}$	2.2180(5)	2.2118(5)	2.260	2.228
d(Ni–C_{ipso})	2.1703(16)	2.1493(16)	2.297	2.174
d(Ni–C_{ortho})	2.4843(16)	2.6595(17)	2.782	2.543
d(Ni–N)	1.8612(14)	1.8507(18)	1.871	1.860
d(N–N)	1.102(2)	1.101(2)	1.111	1.121
$\measuredangle$(P-Ni-P)	120.1	121.4	122.0	118.2
$\Sigma\measuredangle$(C-B-C)	352.6	352.5	350.7	352.7

Density functional theory (DFT) calculations were carried out on **5** to calibrate a method for subsequent electronic-structure calculations.[10] Computations with the B3LYP functional consistently overestimated the Ni–C_{ipso} distance in **5** by approximately 0.1 Å or more (see the Supporting Information). The functional M06L gave far better agreement with the experimentally determined geometry (Table 1) and was chosen for further computations.[11]

Unlike **1**, which under H_2 (1 atm) is in rapid equilibrium with its dihydride form **2** ($K_{obs} \approx 5$; Scheme 3),[6] **5** reacted quantitatively with H_2 over the course of hours to give the pale-orange bridging borohydride–nickel–hydride complex $[(^{Ph}DPB^{iPr})(\mu\text{-H})NiH]$ (**8**). The ^{1}H NMR spectrum of **8** is consistent with a C_s-symmetric molecule at room temperature and features diagnostic resonances in the ^{1}H NMR spectrum at $\delta = -6.65$ and -16.11 ppm corresponding to the bridging and terminal hydride ligands, respectively. In solution, **8** slowly reverted to **5** when stored under N_2. Exposure to a dynamic vacuum also induced H_2 loss from **8**.

The UV/Vis spectrum of **8** exhibits a d–d transition centered around 500 nm with an extinction coefficient of $\varepsilon = 500\,M^{-1}cm^{-1}$. The IR spectrum of **8** featured a prominent absorption at 1814 cm^{-1}, which shifts to 1330 cm^{-1} upon isotopic substitution of D for H, in agreement with its assignment as a Ni–H stretching mode (see Figure S13 in the Supporting Information). DFT calculations predict two stretching modes of similar energy ($\Delta\nu \approx 100\,cm^{-1}$) corresponding to a symmetric and an asymmetric stretch associated with the H–Ni–H unit. The asymmetric stretch was calculated to have an intensity about 20 times larger than that of the higher-energy symmetric stretch. This difference in intensity accounts for our observation of a single feature by IR spectroscopy.

Owing to the slow rate of H_2 activation at the $[(^{Ph}DPB^{iPr})Ni]$ fragment, we could observe the intermediate Ni–(H_2) complex $[(^{Ph}DPB^{iPr})Ni(H_2)]$ (**7**) prior to H–H cleavage. When a solution of **5** in THF was placed under vacuum, the brick-red color ($\lambda_{max} = 479$ nm, $\varepsilon = 2400\,M^{-1}cm^{-1}$) of the N_2 adduct changed to deep blue-green ($\lambda_{max} = 594$ nm, $\varepsilon = 2700\,M^{-1}cm^{-1}$), consistent with N_2 loss to give the THF adduct $[(^{Ph}DPB^{iPr})Ni(THF)]$ (**9**), which is analogous to previously reported $[(^{Ph}DPB^{Ph})Ni(THF)]$.[6] The addition of H_2 gas (1 atm) resulted in an immediate color change to cherry red ($\lambda_{max} = 485$ nm, $\varepsilon = 2600\,M^{-1}cm^{-1}$; Figure 2). The similarity of this absorption to that of **5** is consistent with its attribution to H_2 adduct **7**.

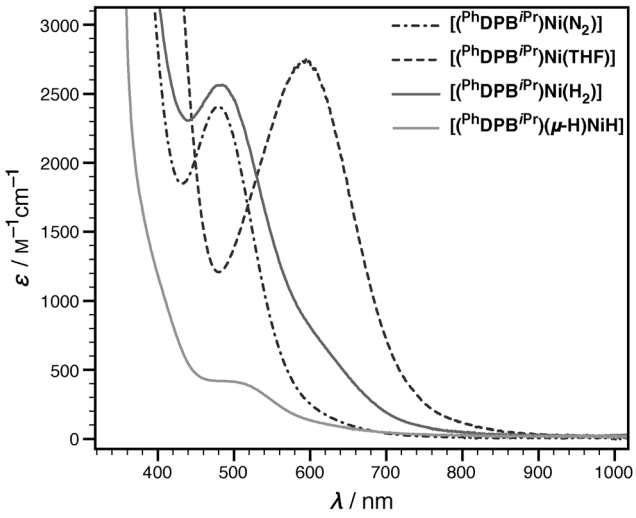

Figure 2. UV/Vis spectra of **5**, **7**, **8**, and **9** in THF.

We carried out NMR spectroscopic studies to verify the presence of an intact H_2 ligand in **7** (Figure 3). Besides a set of resonances corresponding to the $^{Ph}DPB^{iPr}$ ligand framework, a broad singlet at $\delta = -0.97$ ppm was observed by ^1H NMR spectroscopy. When H_2 was replaced with HD, this signal split into a 1:1:1 triplet centered at $\delta = -1.15$ ppm with $^1J_{HD} = 36.5$ Hz, which corresponds to an H–H distance of 0.827 Å on the basis of the empirical relationship established by Luther and Heinekey.[12] At temperatures below −50 °C,

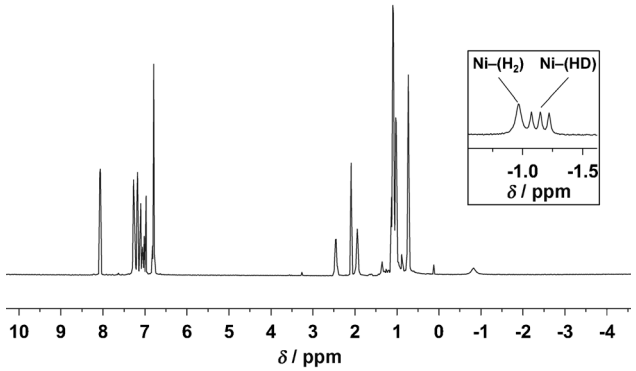

Figure 3. ^1H NMR spectrum of **7** under H_2 (1 atm) in [D_8]toluene. Inset: Part of the ^1H NMR spectrum of **7** under a mixture of H_2 and HD.

a peak corresponding to free H_2 was observed by ^1H NMR spectroscopy, thus indicating that H_2-ligand exchange is slow relative to the NMR time scale at these temperatures. Furthermore, T_1 measurements between −80 and 30 °C established a T_1(min) value for this signal of 20 ms.[13] Taken together, these data support the formulation of **7** as an H_2 adduct of Ni. Although recent computational studies predicted that the nonclassical H_2 adduct is the thermally stable form of complexes of stoichiometry L_2NiH_2 in which L_2 is a chelating diphosphine, no such complex has been experimentally authenticated to date.[14] Complex **7** appears to be a unique example of a d^{10} transition-metal H_2 adduct characterized in solution.[15]

Although **7** has not proven amenable to an X-ray diffraction study, we have examined the complex computationally with density functional theory (M06L/6-311++G**). In accord with the large $^1J_{HD}$ and low T_1(min) values determined experimentally, the DFT-optimized structure of **7** features a short H–H distance (0.8371 Å) characteristic of an intact H_2 ligand. Assignment of the d-electron count of **7** is complicated by the unusual η^2-B,C_{ipso} ligand.[16] Consideration of the borane subunit as a Z-type interaction would indicate a divalent d^8 electronic configuration for Ni according to the covalent bond classification (CBC) method;[17] however, this description proves unsatisfying in some respects. First, the essentially planar boron center renders it distinct from pyramidal borane ligands found in metallaboratrane complexes, in which M→B bonding is inferred.[18] Second, the description of **7** (and related [($^{Ar}DPB^{Ph}$)Ni] complexes[6]) as divalent would situate them as the only tetrahedral diamagnetic d^8 Ni complexes known. In contrast, diamagnetic tetrahedral Ni complexes with a d^{10} configuration are common.[19] Indeed, well-known tetrahedral η^2-olefin complexes of Ni^0, such as [(triphos)Ni(C_2H_4)][20] and [(dmpe)Ni(PPh_3)(η^2-C_2H_4)],[21] provide structural analogues for the binding of the η^2-B,C unit. Given that the utility of a bonding-classification method lies in its ability to group compounds of like electronic structure and reactivity, we favor a zero-valent (d^{10}) description for complexes of the type [($^{Ar}DPB^{R}$)NiL], including **5** and **7**.

The frontier orbitals calculated for **7** further illustrate the suitability of a d^{10} description (Figure 4). Although molecular orbitals corresponding to bonding interactions between Ni and B can be identified (HOMO−2, HOMO−3), they lie in the middle of the d-orbital manifold, higher in energy than a nonbonding orbital clearly of d parentage (HOMO−4).

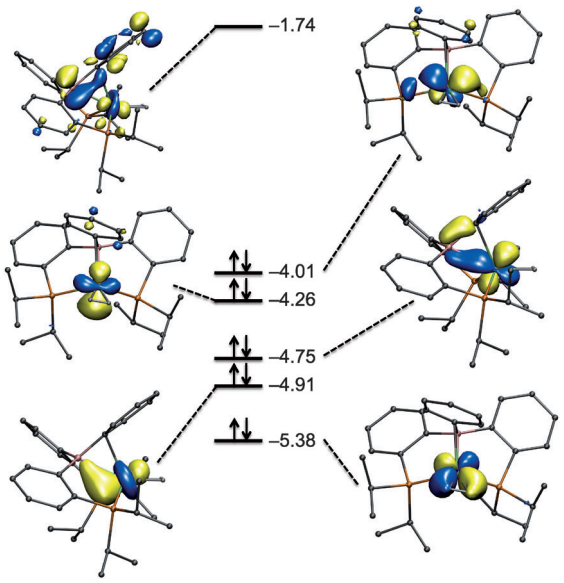

Figure 4. Frontier Kohn–Sham orbitals (LUMO through HOMO−4) calculated for [($^{Ph}DPB^{iPr}$)Ni(H_2)] (M06L/6-311++G**). Orbital energies are given in eV.

Rather than considering the B center of the $^{Ar}DPB^{R}$ framework to be a Z-type ligand, it is better described in the language of the CBC system as Z′,[22] akin to the π-accepting function of a CO ligand but of σ symmetry with respect to the Ni–B vector. In this view, the acceptor function of the B atom is treated as a modest perturbation on a d^{10} tetrahedral ML_4-type electronic structure, that is, a "backbond" (Figure 5).

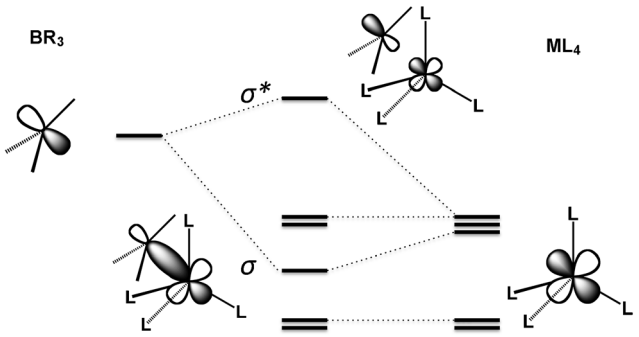

Figure 5. Qualitative molecular-orbital diagram for the interaction between BR_3 and a tetrahedral ML_4 fragment.

Along these lines, the η^2-B,C_{ipso} ligand can be thought of as a polarized alkene within the Dewar–Chatt–Duncanson bonding model,[23] with the donor orbital localized primarily on the carbon atom and the acceptor orbital on the boron atom. To explore this comparison, we optimized a hypothetical complex in which the BPh unit in **7** was replaced with an alkene (C=CH_2) to give **7′** (M06L/6-31 + G*) with a qualitatively identical coordination geometry (see Figure S15 and Table S4 in the Supporting Information). Natural bond orbital (NBO) calculations[24] carried out on **7** and **7′** identified five filled nonbonding d orbitals on Ni in support of a d^{10} (zerovalent) formulation.[25] Second-order perturbation analysis of these natural bond orbitals found an energy associated with Ni(3d)→B(2p) donation of 21.5 kcal mol^{-1} in **7**. An analogous delocalization energy of 45.0 kcal mol^{-1} was identified in **7′** owing to backbonding into the alkene π* orbital ((Ni(3d)→C=C(π*)). These results are consistent with a description of the BPh ligand as both a weaker σ donor and a weaker π acceptor than an alkene. For comparison, analogous calculations on the structurally authenticated Ni^0 olefin complex [(dmpe)Ni(PPh_3)(η^2-C_2H_4)][21] indicated an energy for Ni(3d)→C=C(π*) donation of 41.8 kcal mol^{-1} (see Table S19).

The optimized structures of **7** and **7′** were additionally subjected to atoms-in-molecules[26] (AIM) analysis, which identified (3, −1) bond critical points (BCPs) between the Ni–B (**7**), Ni–C1 (**7′**), and Ni–C2 (**7′**) linkages (see Figure S16). In line with the NBO calculations, the electron densities (Ni–B: 0.067 e bohr^{-3}; Ni–C: 0.099 and 0.097 e bohr^{-3} for **7′**) and the Laplacian of the electron densities (Ni–B: −0.011 e bohr^{-5}; Ni–C: −0.042 and −0.047 e bohr^{-5} for **7′**) at the BCPs indicate that the Ni–B and Ni–C bonds are locally depleted and thus ionic (or dative) in nature (see Table S5).

The above analyses provide a plausible explanation for the relatively strong H_2 binding in **7**. Given the pseudo-*trans* disposition of the B and H_2 ligands, the p orbital on B serves to stabilize the Ni d orbital, which is antibonding with respect to the Ni–(H_2) σ interaction. This description is in keeping with the orbital description of the *trans* influence[27] and has been observed in other systems featuring acceptor interactions with d^{10} metals *trans* to an incoming ligand.[28]

The kinetics of H_2 addition across the Ni–B bond were monitored by ^{1}H NMR spectroscopy (see Figures S4 and S5). At 298 K in C_6D_6 under H_2 (4 atm), **7** decayed by first-order kinetics to give **8** as the sole product with $k = 1.4 \times 10^{-4}$ s^{-1}. The reaction rate was not changed appreciably by reducing the pressure of H_2 to 1 atm. A kinetic isotope effect (k_H/k_D, KIE) of 1.6 was determined, in line with published studies of H–H oxidative addition reactions, which typically exhibit kinetic isotope effects of 1–2.5.[29] These results are consistent with a unimolecular isomerization of the H_2 adduct **7** into dihydride **8**.

By way of comparison, we were able to measure the H_2 addition rate to previously reported **1** as well as the rate of the reverse reaction under equilibrium conditions by two-dimensional magnetization-transfer ^{1}H NMR spectroscopy (2D EXSY).[30] Analysis of the intensities of the diagonal resonances for an exchanging site of interest and the related cross-peaks as a function of the mixing time of the EXSY experiment enabled the measurement of the rate of interconversion of these species. For the system in question, the mesityl aryl hydrogen atoms provide a suitable handle for this analysis, giving pseudo-first-order rate constants for the process of $k_F = 2.0$ s^{-1} and $k_R = 0.45$ s^{-1} under H_2 (1 atm; see the Supporting Information). The analogous H_2 addition reaction for **7** is roughly four orders of magnitude slower.

As the available kinetic data suggested a unimolecular pathway for the conversion of **7** into **8**, we explored the reaction coordinate computationally with a truncated model system (by replacing the isopropyl substituents with methyl groups). We envisioned two likely mechanistic possibilities: one in which oxidative addition of H_2 occurs at Ni, followed by the trapping of Ni–H by B, and one in which the H_2 ligand is activated directly across the Ni–B interaction. We were successful in locating transition structures corresponding to each of these mechanistic hypotheses. A transition state **TS1** corresponding to oxidative addition was located by DFT methods (M06L/6-31 + G*) to connect **7** and **8** (Figure 6a). This transition state has the appearance of a *cis* dihydride, with complete cleavage of the H–H bond ($d_{H-H} = 1.977$ Å). The single imaginary frequency associated with this structure corresponds to a Ni–H bend as the hydride ligand migrates towards boron. This transition state corresponds to a computed activation free energy of 36.9 kcal mol^{-1}. An alternate transition state **TS2** was located in which the B–H bond is formed in concert with H–H bond cleavage (Figure 6b). In contrast to **TS1**, the H–H distance in **TS2** is lengthened to 1.018 Å (versus 0.827 Å in the ground-state H_2 complex), but the H_2 moiety is still essentially intact. Along this pathway, the borane center abstracts hydride from the Ni–(H_2) complex to cleave the H–H bond across Ni. Transition state **TS2**, in which both B and Ni cooperatively cleave H_2, corresponds to a calculated activation energy of 28.1 kcal mol^{-1} and is thus nearly 9 kcal mol^{-1} lower in energy than **TS1**. On the basis of

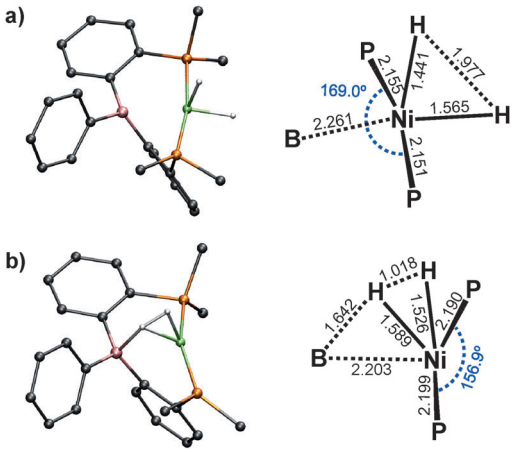

Figure 6. DFT-computed structure of a) **TS1** and b) **TS2** (M06L/6-31+G*) with selected bond lengths [Å] and angles [°] shown at the right. Hydrogen atoms bound to carbon atoms have been omitted for clarity.

these calculations, we favor a mechanism in which both B and Ni interact with the H_2 ligand in the transition state. These findings are consistent with a recent computational study on the reactivity of **1**.[31]

In closing, we have developed a diphosphine–borane-supported Ni fragment, [(^{Ph}DPB^{iPr})Ni], that binds both N_2 and H_2. The H_2 adduct **7** is one of only a few Ni–(H_2) adducts characterized in solution, and to our knowledge, the first transition-metal H_2 adduct featuring a transition-metal center best formulated as d^{10}. The frontier orbitals of **7** highlight a likely role of the borane ligand in stabilizing H_2 binding to the low-valent Ni center. This study thus outlines a strategy in which a multifunctional ligand can enable favorable H_2 binding and oxidative addition at a Ni^0 center.

Received: September 17, 2013
Published online: December 9, 2013

Keywords: borane ligands · H_2 activation · H_2 complexes · nickel · reaction mechanisms

[1] a) E. Bouwman in *Handbook of Homogeneous Hydrogenation*, 1st ed. (Eds.: J. G. de Vries, C. J. Elsevier), Wiley-VCH, Weinheim, **2007**, pp. 93–109; b) C. J. Curtis, A. Miedaner, W. W. Ellis, D. L. DuBois, *J. Am. Chem. Soc.* **2002**, *124*, 1918–1925; c) S. Pfirrmann, S. Yao, B. Ziemer, R. Stößer, M. Driess, C. Limberg, *Organometallics* **2009**, *28*, 6855–6860; d) I. Bach, R. Goddard, C. Kopiske, K. Seevogel, K.-R. Pörschke, *Organometallics* **1999**, *18*, 10–20.

[2] a) G. J. Kubas, *Metal Dihydrogen and σ-Bond Complexes: Structure, Theory, and* Reactivity, 1st ed., Springer, Berlin, **2001**; b) G. J. Kubas, *Chem. Rev.* **2007**, *107*, 4152–4205; c) C. Tsay, J. C. Peters, *Chem. Sci.* **2012**, *3*, 1313–1318; d) S. J. Connelly, A. C. Zimmerman, W. Kaminsky, D. M. Heinekey, *Chem. Eur. J.* **2012**, *18*, 15932–15934.

[3] T. He, N. P. Tsvetkov, J. G. Andino, X. Gao, B. C. Fullmer, K. G. Caulton, *J. Am. Chem. Soc.* **2010**, *132*, 910–911.

[4] a) M. Rakowski DuBois, D. L. DuBois, *Acc. Chem. Res.* **2009**, *42*, 1974–1982; b) F. Gloaguen, T. B. Rauchfuss, *Chem. Soc. Rev.* **2009**, *38*, 100–108.

[5] a) R. H. Morris in *Handbook of Homogeneous Hydrogenation*, 1st ed. (Eds.: J. G. de Vries, C. J. Elsevier), Wiley-VCH, Weinheim, **2007**, pp. 45–70; b) R. M. Bullock in *Handbook of Homogeneous Hydrogenation*, 1st ed. (Eds.: J. G. de Vries, C. J. Elsevier), Wiley-VCH, Weinheim, **2007**, pp. 153–197.

[6] W. H. Harman, J. C. Peters, *J. Am. Chem. Soc.* **2012**, *134*, 5080–5082.

[7] S. Bontemps, G. Bouhadir, P. W. Dyer, K. Miqueu, D. Bourissou, *Inorg. Chem.* **2007**, *46*, 5149–5151.

[8] CCDC 895465 (**4**), and 895466 (**5** and **6**) contain the supplementary crystallographic data for this paper. These data can be obtained free of charge from The Cambridge Crystallographic Data Centre via www.ccdc.cam.ac.uk/data_request/cif.

[9] a) H. Huber, E. P. Kündig, M. Moskovits, G. A. Ozin, *J. Am. Chem. Soc.* **1973**, *95*, 332–344; b) C. A. Tolman, D. H. Gerlach, J. P. Jesson, R. A. Schunn, *J. Organomet. Chem.* **1974**, *65*, C23; c) P. W. Jolly, K. Jonas, C. Krüger, Y.-H. Tsay, *J. Organomet. Chem.* **1971**, *33*, 109–122; d) R. Waterman, G. L. Hillhouse, *Can. J. Chem.* **2005**, *83*, 328–331; e) S. Pfirrmann, C. Limberg, C. Herwig, R. Stösser, B. Ziemer, *Angew. Chem.* **2009**, *121*, 3407–3411; *Angew. Chem. Int. Ed.* **2009**, *48*, 3357–3361; f) D. Zhu, I. Thapa, I. Korobkov, S. Gambarotta, P. H. M. Budzelaar, *Inorg. Chem.* **2011**, *50*, 9879–9887.

[10] Geometry optimizations were performed at the indicated level of theory by using the Gaussian 03 or Gaussian 09 program. Full references are given in the Supporting Information.

[11] a) Y. Zhao, D. G. Truhlar, *Theor. Chem. Acc.* **2007**, *120*, 215–241; b) Y. Zhao, D. G. Truhlar, *Acc. Chem. Res.* **2008**, *41*, 157–167.

[12] T. A. Luther, D. M. Heinekey, *Inorg. Chem.* **1998**, *37*, 127–132.

[13] R. H. Crabtree, *Acc. Chem. Res.* **1990**, *23*, 95–101.

[14] C. Flener Lovitt, G. Frenking, G. S. Girolami, *Organometallics* **2012**, *31*, 4122–4132.

[15] H_2 molecules adsorbed onto Ni and Pd surfaces have been characterized, and a few d^{10} H_2 complexes have been trapped and studied in low-temperature matrices; see Ref. [2b] and references therein.

[16] D. J. H. Emslie, B. E. Cowie, K. B. Kolpin, *Dalton Trans.* **2012**, *41*, 1101–1117.

[17] M. L. H. Green, *J. Organomet. Chem.* **1995**, *500*, 127–148.

[18] H. Braunschweig, R. D. Dewhurst, A. Schneider, *Chem. Rev.* **2010**, *110*, 3924–3957.

[19] F. A. Cotton, G. Wilkinson, C. A. Murillo, M. Bochmann, *Advanced Inorganic Chemistry*, 6th ed., Wiley-VCH, Weinheim, **1999**.

[20] J. Mautz, K. Heinze, H. Wadepohl, G. Huttner, *Eur. J. Inorg. Chem.* **2008**, 1413–1422; triphos = 1,1,1-tris(diphenylphosphanylmethyl)ethane.

[21] K. R. Porschke, R. Mynott, C. Kruger, M. J. Romao, *Z. Naturforsch. B* **1984**, *39*, 1076–1081; dmpe = 1,2-bis(dimethylphosphanyl)ethane.

[22] G. Parkin in *Comprehensive Organometallic Chemistry III* (Eds.: R. H. Crabtree, D. M. P. Mingos), Elsevier, Oxford, **2006**, pp. 1–57.

[23] J. Chatt, L. A. Duncanson, *J. Chem. Soc.* **1953**, 2939–2947.

[24] F. Weinhold, C. R. Landis, *Valency and Bonding: A Natural Bond Orbital Donor-Acceptor Perspective*, Cambridge University Press, Cambridge, UK, **2005**.

[25] See also a related σ-borane d^{10} Ni complex: M. G. Crestani, M. Muñoz-Hernández, A. Arévalo, A. Acosta-Ramírez, J. J. García, *J. Am. Chem. Soc.* **2005**, *127*, 18066–18073.

[26] R. F. W. Bader, *Atoms in Molecules: A Quantum Theory*, Oxford University Press, Oxford, **1994**.

[27] M. P. Mitoraj, H. Zhu, A. Michalak, T. Ziegler, *Int. J. Quantum Chem.* **2009**, *109*, 3379 – 3386.
[28] T.-P. Lin, R. C. Nelson, T. Wu, J. T. Miller, F. P. Gabbaï, *Chem. Sci.* **2012**, *3*, 1128 – 1136.
[29] T. Hascall, D. Rabinovich, V. J. Murphy, M. D. Beachy, R. A. Friesner, G. Parkin, *J. Am. Chem. Soc.* **1999**, *121*, 11402 – 11417, and references therein.
[30] E. W. Abel, T. P. J. Coston, K. G. Orrell, V. Sik, D. Stephenson, *J. Magn. Reson.* **1986**, *70*, 34 – 53.
[31] G. Zeng, S. Sakaki, *Inorg. Chem.* **2013**, *52*, 2844 – 2853.

